19th Australasian Fluid Mechanics Conference
Melbourne, Australia
8-11 December 2014

Regions of Uniform Streamwise Momentum in Turbulent Boundary Layers

C. M. de Silva, I. Marusic and N. Hutchins

[1]Department of Mechanical Engineering, The University of Melbourne, Victoria 3010, Australia.

Abstract

This study investigates the presence of zones of uniform streamwise momentum (or UMZs) across a range of Reynolds numbers in turbulent boundary layers, spanning more than an order of magnitude ($Re_\tau \approx 10^3 - 10^4$). A rigorous examination of the identification criteria suggested by Adrian *et al.* [1] is presented, and then employed to show that a zonal-like structure is prevalent in all datasets examined. Preliminary observations reveal further evidence of a hierarchical length scale distribution of structures within turbulent boundary layers, leading to zonal-like organisations. Interpretation of these results is aided by employing synthetic velocity fields generated using the attached-eddy model. The characteristics of the UMZs present the model generated velocity fields are shown to qualitatively match well with experimental results.

Introduction

The inhomogeneous nature of wall-turbulence lends itself to the characterisation of the turbulence into structures, eddies or coherent motions. Recent summaries on these structural features are discussed by Marusic and Adrian [7] and Herpin *et al.* [5]. A distinct feature reported in previous studies is the existence of large and irregularly shaped regions of uniform streamwise momentum (hereafter referred to as uniform momentum zones, or UMZs). The presence of UMZs were first reported by Meinhart and Adrian [8], using particle image velocimetry (PIV) on a streamwise (x), wall-normal (z) measurement plane. This zonal-like structural arrangement is best described with reference to figure 1, where a randomly selected streamwise velocity field ($\widetilde{U}^+$) on a $x-z$ plane is shown. Qualitatively, two regions of relatively uniform streamwise momentum are observed, labelled ① and ②, with sharp shear layers existing between these regions.

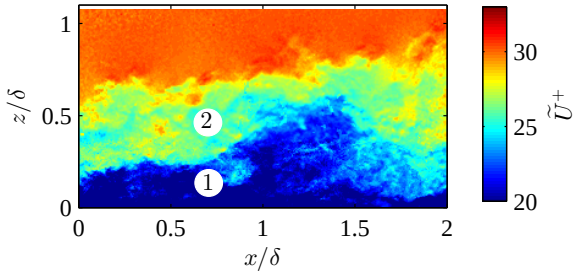

Figure 1. Colour contours of streamwise velocity ($\widetilde{U}^+$) at $Re_\tau \approx 8000$ from a single PIV frame. For this example two possible UMZs are observed, labelled ① and ②.

Encouraged by the observed presence of UMZs, Adrian *et al.* [1] conducted an extensive study on these features using high resolution PIV datasets in the $x-z$ plane. Several significant observations were made in this study across all Reynolds numbers considered ($350 < Re_\tau < 2000$). They showed that UMZs are persistent for large streamwise lengths, on the order of the boundary layer thickness (δ). Consequently, one would expect UMZs to have a significant contribution to the structural organisation in a turbulent boundary layer. It was postulated that these UMZs were closely linked with groups of hairpins, which typically consist of seven or more hairpins spanning over large streamwise lengths of $O(\delta)$. Qualitative observations showed that UMZs are inclined at 12° (on average, varying between $3-35°$) to the wall. Following Adrian *et al.* [1], Tomkins and Adrian [12] performed a set of experiments on a $x-y$ plane. Here, the dominant motions were shown to be large scale low-momentum zones elongated in the streamwise direction, which are bordered by organised vortices. These results offered further support for the zonal-like structure in turbulent boundary layers.

The present study aims to analyse UMZs in turbulent boundary layers using both experimental data and the attached-eddy model. First, we examine a detection criteria for UMZs and re-establish prior observations. Thereafter, the presence of UMZs is investigated using recent experimental datasets spanning over a decade of Reynolds numbers.

Experimental Setup

The present study utilises PIV databases, all acquired using planar $x-z$ orientations across a range of Reynolds numbers from $Re_\tau \approx 1200 - 14500$. Key experimental parameters of the databases are summarised in table 1. Further details on each dataset can be found in their respective publications.

The analysis to follow relies on PIV datasets with adequate spatial resolution and dynamic spatial range. Achieving this is challenging for high Reynolds numbers since the range of scales of turbulent motions becomes large. Therefore, the high Reynolds number datasets employed in the present study utilise a unique experimental configuration with multiple cameras to obtain both a large field of view (streamwise extent $> 2\delta$) with targeted spatial resolution where it is most critical (closer to the wall). The imaging system consists of eight PCO4000 cameras (4008×2672 pixels, 2Hz) arranged in two horizontal rows (bottom and top), giving a combined resolution of over 90 megapixels. The spatial resolution based on the interrogation window size varies between the bottom (pixel size of 60μm) and top (pixel size of 100μm) cameras due to different magnification levels. However, we attain a vector spacing on the order of the Kolmogorov scale (η) across the entire extent of the boundary layer at an overlap of 50% based on the bottom cameras. We note that the image particle diameter, seeding density and particle displacement cannot be optimised for each magnification level simultaneously. Instead, a compromise is made when choosing these parameters to obtain reasonable accuracy at all magnification levels. Further details on the experimental setup can be found in de Silva *et al.* [3].

Experiment	Re_τ	$L_x \times L_z$	$\Delta x^+, \Delta z^+$
Hambleton *et al.* [4]	1200	$1.5\delta \times 1.3\delta$	16×16
de Silva *et al.* [3]	8000	$2\delta \times 1.1\delta$	20×20
de Silva *et al.* [3]	14500	$2\delta \times 1.1\delta$	20×20

Table 1. Experimental parameters of the three PIV databases employed. L_x and L_z correspond to the streamwise and wall-normal extent of the field of view, respectively. Δx^+ and Δz^+ correspond to the vector spacing. All datasets consist of over a thousand independent PIV frames.

Processing

The experimental data at $Re_\tau \approx 8000$ and $Re_\tau \approx 14500$ are processed using an in-house PIV package [3]. To summarise, an interrogation window size of approximately 40 (32×32 pixels) and 90 (48×48 pixels) viscous units is used for the bottom and top cameras, respectively at $Re_\tau = 8000$. In order to closely match the spatial resolution across the Reynolds numbers studied, the interrogation window sizes are halved at the higher Reynolds number studied. Furthermore, to maintain uniform vector spacing across the entire field of view (FOV), the vector grid in real space is determined with an overlap of 50% for the bottom cameras via a calibration process, after which the vector spacing for the top cameras is matched to the bottom cameras.

In order to capture a large FOV, lower magnification levels are employed, which compromises the particle image size. This leads to a pixel-locking in the dataset [2]. The detection criteria employed to detect UMZs (to be discussed further) is sensitive to any pixel-locking in PIV datasets, therefore it is necessary to minimise this bias error. First, a filter based on a Gaussian kernel is applied on the raw images, which has been shown to reduce the severity of pixel-locking [2]. Furthermore, an interrogation window deformation approach is adopted during the cross-correlation phase, which is also known to reduce the influence of pixel-locking [11]. In addition, we employ a technique detailed in Roth and Katz [10] (commonly referred to as matched histogram thresholding or MHE), which minimises any residual pixel-locking. Figure 2 shows the pdf of $\widetilde{U}$ at $Re_\tau \approx 8000$ for the range $0 < z^+ < 0.5\delta$ across all PIV frames. The dashed red line (−−) shows the extent of the pixel-locking bias in the dataset. The solid red line (–) shows results after employing a Gaussian kernel on image pairs in conjunction with an interrogation window deformation during PIV processing. Results show a significant reduction in pixel-locking. Consequently, the MHE technique only has a subtle effect as shown by the solid blue line (–).

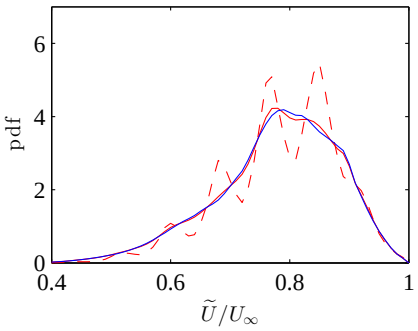

Figure 2. Pdf of streamwise velocity ($\widetilde{U}$) at $Re_\tau \approx 8000$ within the range $0 < z^+ < 0.5\delta$ across all PIV frames. Dashed and solid red lines (−− and –) correspond to dataset obtained before and after using a Gaussian kernel on image pairs and interrogation window deformation. Solid blue line (–) corresponds to dataset after utilising the pixel-locking corrections.

Detection Criteria

Following Adrian *et al.* [1] and the definition of a UMZ (extended region of low streamwise velocity fluctuations) we utilise the pdf of the streamwise velocity component to detect the presence of local maxima. These local maxima on the pdf and their associated streamwise velocity magnitude (commonly referred to as a modal velocity) represents the streamwise momentum of possible UMZs. Since the procedure to detect UMZs relies on the pdf of the streamwise velocity, the streamwise extent of the velocity field utilised to compute the pdf ($\mathcal{L}_x$) plays an important role. This influence of $\mathcal{L}_x$ is best illustrated with reference to figure 3, where (a) shows a sample velocity field spanning 2δ obtained at $Re_\tau \approx 8000$ (grey-scale colour map) with the included region shown using colour contours ($\approx 0.01\delta$). The corresponding histogram of the streamwise velocity is shown in figure 3(b). The peaks of this pdf correspond to possible modal velocities ($\widetilde{U}_\mathrm{m}$, indicated by ∘ symbols). Figure 3 (c-d) is a reproduction of the same result at $\mathcal{L}_x \approx 0.5\delta$. Qualitatively, a streamwise domain length of 0.01δ shows several peaks, meanwhile at $\mathcal{L}_x \approx 0.5\delta$ two distinct peaks (or modal velocities) are observed on the pdf of the streamwise velocity and the corresponding UMZs are also identifiable by visually inspecting figure 3(c).

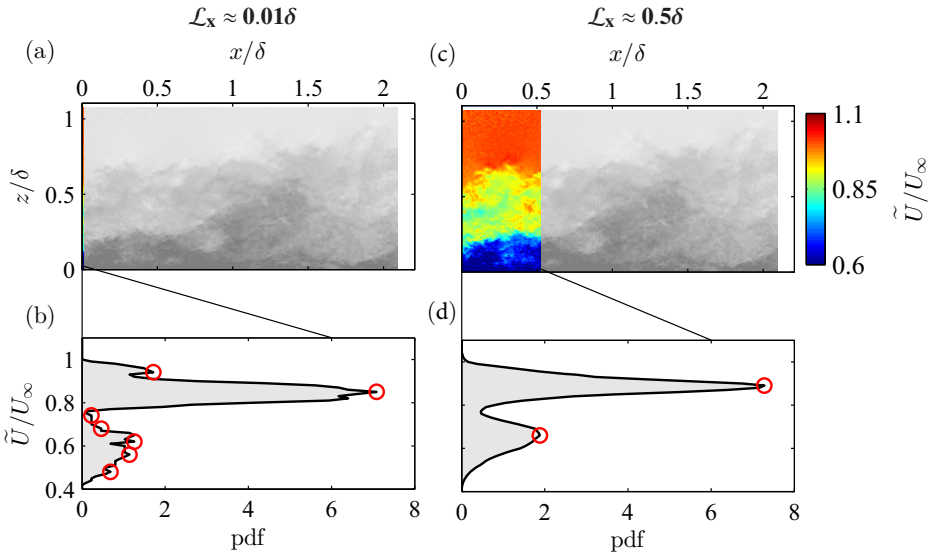

Figure 3. Influence of streamwise domain length ($\mathcal{L}_x$) on the number of detected modal velocities detected. (a) and (c) iso-contours of streamwise velocity ($\widetilde{U}$) of the included region of a single PIV frame (colour), and omitted region in gray-scale. (b) and (d) pdf of $\widetilde{U}/\delta$ constructed using included region indicated in (a) and (c), respectively. The (∘) symbols indicate the detected modal velocities. (a-b) corresponds to $\mathcal{L}_x \approx 0.01\delta$ and (c-d) corresponds to $\mathcal{L}_x \approx 0.5\delta$ at $Re_\tau \approx 8000$.

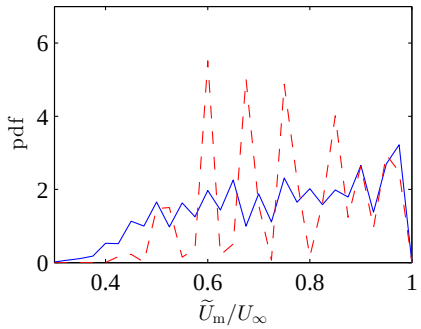

Figure 4. Pdf of modal velocities ($\widetilde{U}_m$) found in all PIV frames at $Re_\tau \approx 8000$. Dashed (– –) and solid (–) lines corresponds to dataset obtained before and after minimising any pixel-locking.

We note that the large number of peaks detected at $\mathcal{L}_x \ll 0.5$, is primarily caused by the limited number of grid points in z in the velocity field, and should not be simply considered as spurious detections. Consequently, we require a larger $\mathcal{L}_x$ to obtain sufficient samples for the pdf. This procedure introduces an implicit filter which inhibits the detection of UMZs encompassing small spatial regions ($\mathcal{L}_x \ll 0.5$). Nevertheless, our results show that UMZs which are clearly identifiable are detected by the described procedure when $\mathcal{L}_x \approx 0.5\delta - 1\delta$. We also note that this range is comparable to that employed by Adrian *et al.* [1] where $\mathcal{L}_x = 1.2\delta$, which corresponded to the streamwise extent of their FOV. Therefore for all subsequent analysis, we employ a streamwise domain length of $\mathcal{L}_x \approx 0.5\delta$ for detecting UMZs in all datasets considered. Further analysis would be necessary to carefully examine the influence of $\mathcal{L}_x$, perhaps by employing synthetic velocity fields where the number of UMZs are known a-priori.

As a final note, it is worth highlighting the influence of a pixel-locked PIV dataset on the detected modal velocities. Figure 4 shows a pdf of $\widetilde{U}_m$ across all PIV frames at $Re_\tau \approx 8000$. The dashed line corresponds to a pdf of $\widetilde{U}_m$ prior to implementing the techniques discussed previously to minimise any pixel-locking. Here, we observe a series of peaks that should be considered as spurious, since they are caused by $\widetilde{U}_m$ being biased towards integer pixel displacements. The solid line in figure 4 corresponds to results after minimising any residual pixel-locking, where the spurious peaks are now suppressed, thus indicating that the bias towards integer pixel displacements of $\widetilde{U}_m$ is minimal.

Assessment of Detection Criteria

An assessment of the detection criteria for UMZs is conducted by utilising a dataset at $Re_\tau = 1200$ [4]. This dataset is chosen for this purpose since it has a comparable Reynolds number to prior work [1], thereby enabling us to draw comparisons to prior observations. Furthermore, we can comment on whether the observations are universal across independent datasets from different facilities and at a different $\mathcal{L}_x$. Figure 5 shows pdfs of the streamwise velocity component from randomly chosen PIV images at $Re_\tau \approx 1200$ where the ○ symbols correspond to the detected modal velocities. Similar to the qualitative manual approach employed by Adrian *et al.* [1], we observe three UMZs ($N_{UMZ} \approx 3$) on average at an equivalent Re_τ.

Uniform Momentum Zones at High Reynolds Numbers

This section aims to apply the established detection criteria on the experimental databases at $Re_\tau \approx 8000$ and $Re_\tau \approx 14500$. Preliminary qualitative comparisons between pdfs of streamwise velocity at the range of Reynolds numbers considered show

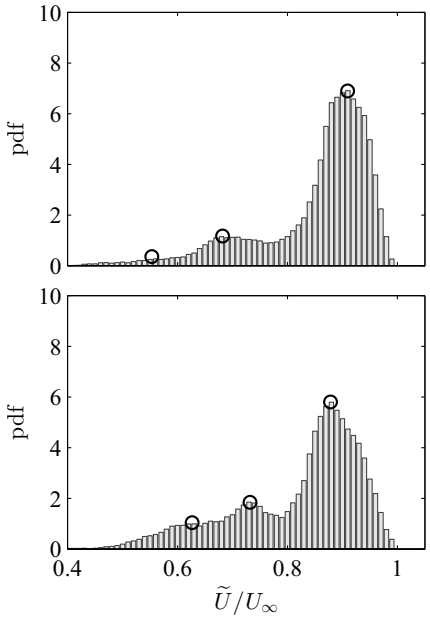

Figure 5. Pdfs of the instantaneous streamwise velocity normalised by $\widetilde{U}/U_\infty$ with a streamwise domain length of 0.5δ at $Re_\tau \approx 1200$. Each pdf corresponds to a randomly chosen PIV frame with ○ corresponding to the detected modal velocities.

an increase in the number of detected UMZs (N_{UMZ}) with increasing Re_τ (see figures 5 ($Re_\tau \approx 1200$), 6a ($Re_\tau \approx 8000$)). We note that examples at $Re_\tau \approx 14500$ are not reproduced here for brevity. Previously, Adrian *et al.* [1] observed no variation in N_{UMZ} from $Re_\tau = 355$ to $Re_\tau = 2000$, however, this may be caused by the limited range and magnitude of Re_τ considered. The present study considers a range of Re_τ spanning over a decade, enabling us to better discern if such a trend exists.

The corresponding instantaneous streamwise velocity field is shown in figure 6(b). The boundaries/edges of each detected UMZ are represented by solid lines (–), which are overlaid on colour contours of streamwise velocity. These boundaries are approximated as the mid-point between each pair of modal velocities. Qualitatively the zonal-like structure is easily observable and it is evident that the edges of UMZs are flanked by a sudden change in streamwise velocity in the wall-normal direction (high $\partial\widetilde{U}/\partial z$). We note that these observations are repeatable in almost any PIV frame considered from all three PIV databases employed, thus providing a certain degree of validity to the approach used to detect the edges of UMZs.

Attached-Eddy Model

The models described in the work of Perry and co-workers (see Perry and Chong [9]) based on the attached-eddy hypothesis have been shown to reasonably reproduce flow statistics of wall-bounded turbulence. To compliment the experimental databases employed in this study, synthetic velocity fields (hereafter referred to as AEH velocity fields) are generated using a similar model to that described in Marusic [6] where hierarchies of packets (each of which consist of several hairpins) are randomly distributed.

A qualitative comparison between an experimental velocity field at $Re_\tau \approx 8000$ (see figure 1) and a synthetic velocity field at $Re_\tau = 6400$ (shown in figure 7) chosen randomly shows good agreement, providing further validity to the attached eddy model from a spatial representation perspective. One notable difference is the lack of small scale activity away from the wall

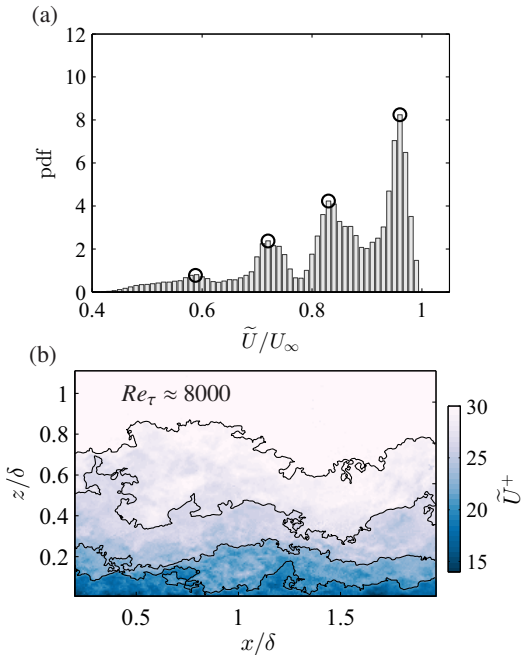

Figure 6. (a) Figure 5 reproduced at $Re_\tau \approx 8000$. (b) Edges of UMZ determined using modal velocities overlaid on colour contours of streamwise velocity ($\widetilde{U}$) from a single PIV frame at $Re_\tau \approx 8000$.

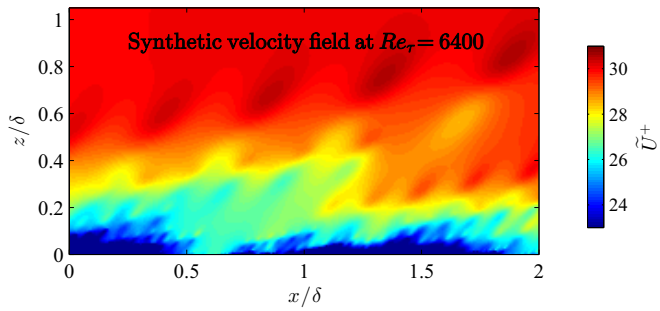

Figure 7. Colour contours of streamwise velocity ($\widetilde{U}^+$) at (a) $Re_\tau \approx 8000$ from a single PIV frame, (b) $Re_\tau = 6400$ from a synthetic velocity field generated using packets of hairpins.

in the synthetic velocity fields due to the nature of how they are generated, where eddy sizes follow a geometric progression based on the distance from the wall. Nevertheless, the zonal-like structural organisation is easily observable in the velocity fields from the model. Although not reproduced here, the statistical behaviour of the detected UMZs in the AEH velocity fields is quantitatively comparable to that observed from the experimental datasets.

Conclusions

This paper analyses the existence of large, irregularly shaped regions of uniform streamwise momentum in turbulent boundary layers. A detection criterion described by Adrian *et al.* [1] using the probability density histograms of the streamwise velocity is extended for large datasets, and is shown to accurately detect UMZs (and their associated modal velocities). Selecting an appropriate streamwise domain length ($\mathcal{L}_x$) to compute the pdf of the streamwise velocity is shown to be important to the process of extracting UMZs. This detection scheme is applied to three datasets spanning over a decade of Reynolds numbers. Preliminary results show an increase in the number of detected UMZs with increasing Reynolds number. An extension of the current analysis may provide further evidence of a hierarchical length scale distribution of structures within the boundary layer. These observations are supported through analysis of synthetic velocity fields generated with the attached-eddy model. The presence of UMZs and their characteristics from the generated synthetic fields are shown to be qualitatively similar to results obtained experimentally.

Acknowledgements

The authors gratefully thank the financial support of the Australian Research Council.

References

[1] Adrian, R. J., Meinhart, C. D. and Tomkins, C. D., Vortex organization in the outer region of the turbulent boundary layer, *J. Fluid Mech.*, **422**, 2000, 1–54.

[2] Adrian, R. J. and Westerweel, J., *Particle Image Velocimetry*, Cambridge University Press, 2011.

[3] de Silva, C. M., Gnanamanickam, E., Atkinson, C., Buchmann, N. A., Hutchins, N., Soria, J. and Marusic, I., High spatial range velocity measurements in a high Reynolds number turbulent boundary layer, *Phys. Fluids*, **26**, 2014, 025117.

[4] Hambleton, W. T., Hutchins, N. and Marusic, I., Simultaneous orthogonal-plane particle image velocimetry measurements in a turbulent boundary layer, *J. Fluid Mech.*, **560**, 2006, 53–64.

[5] Herpin, S., Stanislas, M., Foucaut, J. M. and Coudert, S., Influence of the Reynolds number on the vortical structures in the logarithmic region of turbulent boundary layers, *J. Fluid Mech.*, **716**, 2013, 5–50.

[6] Marusic, I., On the role of large-scale structures in wall turbulence, *Phys. Fluids*, **13**, 2001, 735.

[7] Marusic, I. and Adrian, R. J., The eddies and scales of wall turbulence, in *Ten Chapters in Turbulence*, editors P. A. Davidson, K. Yukio and K. R. Sreenivasan, Cambridge University Press, 2012.

[8] Meinhart, C. D. and Adrian, R. J., On the existence of uniform momentum zones in a turbulent boundary layer, *Phy. Fluids*, **7**, 1995, 694.

[9] Perry, A. E. and Chong, M. S., On the mechanism of wall turbulence, *J. Fluid Mech*, **119**, 1982, 106–121.

[10] Roth, G. and Katz, J., Five techniques for increasing the speed and accuracy of PIV interrogation, *Meas. Sci. Technol.*, **12**, 2001, 238–245.

[11] Scarano, F., Iterative image deformation methods in PIV, *Meas Sci Tech.*, **13**, 2001, R1–19.

[12] Tomkins, C. D. and Adrian, R. J., Spanwise structure and scale growth in turbulent boundary layers, *J. Fluid Mech.*, **490**, 2003, 37–74.